

Double K -shell-vacancy production in the decays of ^{181}W and ^{165}Er

C. W. E. van Eijk, J. P. Wagenaar, F. Bergsma, and W. Lourens
Physics Department, Delft University of Technology, Delft, The Netherlands

(Received 27 April 1982)

The probabilities P_{KK} of double- K -shell-vacancy production per K -electron-capture decay of ^{181}W and ^{165}Er have been determined by means of $K\alpha$ x-ray- K x-ray coincidence experiments: $P_{KK}=(2.4\pm 0.6)\times 10^{-6}$ and $P_{KK}=(8.2\pm 2.8)\times 10^{-6}$, respectively. The observed energy shifts of the hypersatellite $\text{Ta}K\alpha_1^H$ x-ray and $\text{Ho}K\alpha_1^H$ x-ray lines are 1026 ± 62 eV and 930 ± 70 eV, respectively. In the case of ^{181}W , the theoretical P_{KK} value deviates significantly from the above-mentioned experimental value. In combination with results from other experiments, this strongly suggests that, contrary to what the present theory predicts, P_{KK} shows a considerable dependence on the ratio of transition energy to threshold energy.

I. INTRODUCTION

The theory which predicts values for P_{KK} , the probability of double K -shell-vacancy production per K -electron-capture (EC) decay, has been developed during the last four decades. Recent reviews have been presented by Intemann¹ and Bambynek *et al.*² The most advanced calculations are those by Intemann¹ and by Mukoyama *et al.*³ Intemann's calculations result in values for $P_{KK}(\text{SO})$, the "shakeoff" probability, whereas those of Mukoyama *et al.* result in values for both $P_{KK}(\text{SO})$ and $P_{KK}(\text{SU})$, the "shakeup" probability. The terms shakeoff and shakeup refer to the transition of the noncaptured K -shell electron to, respectively, a continuum state and an unoccupied bound state as the result of the sudden change in the central potential due to the EC process [$P_{KK}=P_{KK}(\text{SO})+P_{KK}(\text{SU})$].

From an experiment, recently performed on ^{109}Pd and ^{109}Cd (Ref. 4), the conclusion has been drawn that the P_{KK} values calculated by Mukoyama *et al.* might be too large for EC decays with a decay energy close to the threshold energy for the production of two K -shell vacancies, i.e., an energy of approximately twice the K -binding energy. In an attempt to draw a more definite conclusion, we performed a measurement of P_{KK} on ^{181}W ($t_{1/2}=121$ d). This isotope disintegrates by EC to ^{181}Ta : to 34% to an excited state at 6 keV and to 66% to the ground state.⁵ For these disintegrations the ratio of the decay energy to the threshold energy is about 1.4. This ratio is smaller than the ratio for any case studied so far. For comparison, we also measured P_{KK} for the EC decay of ^{165}Er to the ground state of ^{165}Ho ($t_{1/2}=10.4$ h). For this decay, the ratio of the decay energy to the threshold energy is 3.3. The

results of the measurements are presented in the following sections.

II. METHOD OF MEASUREMENT

The P_{KK} 's have been determined from coincidence measurements between hypersatellite $K\alpha_1^H$ x rays and satellite K^S x rays. A hypersatellite K^H x ray is emitted when the first of the two K -shell vacancies is filled ($K^{-2}\rightarrow K^{-1}X^{-1}$); a satellite K^S x ray is emitted when the second K -shell vacancy is filled ($K^{-1}X^{-1}\rightarrow Y^{-1}X^{-1}$).

K^H x rays have a higher energy than diagram K x rays. In the case of ^{181}W the energy difference between the $\text{Ta}K\alpha_1^H$ x rays and the diagram $K\alpha_1$ x rays is 996 ± 12 eV, as can be found from an interpolation of data obtained from experiments on other isotopes.⁶ In the case of ^{165}Er the corresponding difference is 873 ± 10 eV. Satellite K^S x rays also have a higher energy than diagram K x rays. In the case of ^{181}W the energy difference between $\text{Ta}K\alpha_1^S$ x rays and diagram $K\alpha_1$ x rays is ~ 120 eV for $K^{-1}L^{-1}\rightarrow L^{-2}$.⁷ For $K^{-1}M^{-1}\rightarrow L^{-1}M^{-1}$ the difference is negligibly small. For ^{165}Er , the shift of the $\text{Ho}K\alpha_1^S$ line is ~ 105 eV for $K^{-1}L^{-1}\rightarrow L^{-2}$.

The $K\alpha_1^H$ x rays were measured in a 25-mm² intrinsic-Ge x-ray detector manufactured by Princeton Gamma-Tech. The energy resolution of this detector is ~ 400 eV full width at half maximum (FWHM) in the energy region of interest, which offers the possibility of observing the Ta and the $\text{Ho}K\alpha_1^H$ x-ray lines well-separated from the Ta and the Ho diagram $K\alpha_1$ x-ray lines, respectively. The $K\alpha_2^H$ lines are obscured by the diagram $K\alpha_1$ lines. For this reason, we confined ourselves to the $K\alpha_1^H$ lines for the determination of the P_{KK} 's.

The K^S x rays were measured in a 40-mm-diam, 5-mm-thick, NaI(Tl) x-ray crystal. A coincidence circuit was employed with time-window values between 40 and 80 ns. The Ge coincidence spectrum, accidental-coincidence spectrum and singles spectrum were recorded simultaneously by means of a routing system. In addition, in a number of measurements we also recorded the NaI(Tl) spectrum and the time spectrum. The data were handled by means of a PDP 11/10 computer with a CAMAC interface.

The ^{181}W activity was obtained from neutron bombardment of ^{180}W (enrichment 93 at. %) for 24 hours at a neutron flux of $2.5 \times 10^{14} \text{ cm}^{-2} \text{ s}^{-1}$. Sources were prepared by the evaporation of a drop of active solution on Scotch tape. A source was sandwiched between the two detectors placed at 180° . In order to prevent the detection of Auger electrons and electrons arising from double K -shell-vacancy production, Al foils of 0.3-mm thickness were placed on either side of a source. We used two sources with strengths between 100 and 500 nCi.

The ^{165}Er activity was obtained from neutron bombardment of $^{164}\text{Er}_2\text{O}_3$ (enrichment 74 at. %) for 12 hours at a neutron flux of $\sim 1 \times 10^{13} \text{ cm}^{-2} \text{ s}^{-1}$. In order to reduce the contamination with ^{171}Er ($t_{1/2} = 7.5 \text{ h}$) we introduced a waiting time of three days. In this period a separation of rare-earth elements was performed in a Dowex 50 ion-exchange column at 50°C with 0.75-M phosphoric acid as eluant; the length of the column was 120 mm, the diameter 8 mm.⁸ As ^{169}Yb ($t_{1/2} = 32 \text{ d}$) was the main contaminant, natural Yb was added as a carrier. After the three-day period, two sources were prepared. Each source was used for ~ 20 hours. The source strengths were between ~ 500 and ~ 100 nCi during the measurements. The irradiations were organized in such a way that four sources were available per week. The sources were mounted in the same way as the ^{181}W sources.

For ^{181}W the following relation is found between P_{KK} , N_c , the number of $\text{Ta}K\alpha_1^H$ x-ray counts in the coincidence spectrum recorded with the Ge detector and N_{NaI} , the number of $\text{Ta}K$ x-ray counts in a gate set on the K x rays recorded with the NaI(Tl) detector:

$$P_{KK} = \frac{1}{\alpha_1 \omega_K} \frac{N_c}{\epsilon_c \epsilon_{\text{Ge}} N_{\text{NaI}}}, \quad (1)$$

where ϵ_c is the coincidence efficiency, ϵ_{Ge} is the product of the detection efficiency and the solid angle of the Ge detector, α_1 is the $K\alpha_1$ x-ray fraction of all the $\text{Ta}K$ x rays, and ω_K is the fluorescence yield for $\text{Ta}K$ x rays. In the derivation of this for-

mula it has been assumed (1) that the fluorescence yields ω_K^S of K^S x rays, ω_K^H of K^H x rays, and ω_K of diagram K x rays are identical, and (2) that α_1^H , the fraction of $K\alpha_1^H$ x rays of all the K^H x rays, is identical with α_1 . Justification of these assumptions is found in Ref. 9. Furthermore, we neglected K x rays from internal conversion of the 136-keV and 159-keV transitions in Ta (EC branching ratios to these levels are 0.11% and 0.23%, respectively; no K EC).

Formula (1) is also applicable to the case of ^{165}Er if we read $\text{Ho}K$ x rays instead of $\text{Ta}K$ x rays.

The instrumental constant $\epsilon_c \epsilon_{\text{Ge}}$ has been determined by means of coincidence measurements on ^{159}Dy ($t_{1/2} = 144 \text{ d}$) and ^{195}Au ($t_{1/2} = 183 \text{ d}$) calibration sources.⁵ The ^{159}Dy activity was obtained from neutron bombardment of $^{158}\text{Dy}_2\text{O}_3$ (enrichment 21 at. %) for six days at a neutron flux of $\sim 1 \times 10^{13} \text{ cm}^{-2} \text{ s}^{-1}$. For the ^{195}Au source we used commercially available carrier-free ^{195}Au with a specific activity of more than 100 μCi per μg of Au. The sources were made in the same way as the ^{181}W sources and had strengths between 100 and 500 nCi. They were sandwiched between 0.3-mm Al foils and placed in the same position as the ^{181}W and ^{165}Er sources.

Coincidence measurements on a ^{159}Dy source result in values for $\epsilon_c \epsilon_{\text{Ge}}$ at 45.5 keV ($\text{Tb}K\alpha$ x rays), 50.3 keV ($\text{Tb}K\beta$ x rays), and 58 keV (γ rays); a ^{195}Au source gives $\epsilon_c \epsilon_{\text{Ge}}$ values at 31 keV (γ rays), 66 keV ($\text{Pt}K\alpha$ x rays), 76 keV ($\text{Pt}K\beta$ x rays), and 99 keV (γ rays). From the singles spectra we obtained relative ϵ_{Ge} values at these energies. The coincidence efficiency ϵ_c was found to be constant at energies larger than ~ 40 keV. For the $\text{Ho}K\alpha_1^H$ x rays ($E = 48.5 \text{ keV}$) and the $\text{Ta}K\alpha_1^H$ x rays ($E = 58.5 \text{ keV}$) we thus obtained, respectively, $\epsilon_c \epsilon_{\text{Ge}} = (1.18 \pm 0.07) \times 10^{-2}$ and $\epsilon_c \epsilon_{\text{Ge}} = (1.10 \pm 0.07) \times 10^{-2}$. The errors are mainly due to the uncertainties in the decay schemes⁵ and in the summation corrections ($\sim 11 \pm 5\%$).

III. RESULTS AND DISCUSSION

We performed two series of measurements on ^{181}W . Each series took approximately 1000 h. Calibration measurements were performed about every 200 h. Between the two series we measured on ^{165}Er . We used 10 sources (total measuring time 200 h; see Sec. II) and performed one calibration per source.

Figure 1 shows the $\text{Ta}K\alpha$ x-ray region of the coincidence spectrum, recorded with the Ge detec-

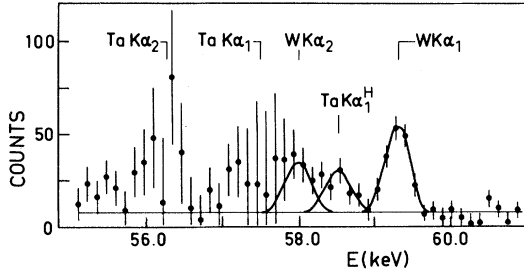


FIG. 1. Ge coincidence spectrum of the Ta $K\alpha$ x-ray region recorded in the first series. Random coincidences have been subtracted.

tor in the first series. Ta diagram $K\alpha$ x-ray random coincidences have been subtracted. The contamination with $W K\alpha$ x rays is due to ^{182}Ta ($t_{1/2} = 115$ d), which is produced by neutron capture in ^{181}Ta . The shapes of the $W K\alpha$ lines shown in Fig. 1 have been obtained from a separate coincidence measurement on a ^{182}Ta source. Between the two $W K\alpha$ lines the $\text{Ta} K\alpha_1^H$ line shows up clearly. Its content is $N_c = 73 \pm 22$ counts. The error is a one-sigma value. The results of the two series of measurements on ^{181}W have been summarized in Table I. We used $\alpha_1 \omega_K = 0.48$ (Ref. 10) for ^{181}W as well as for ^{165}Er .

Figure 2 shows the $\text{Ho} K\alpha$ x-ray region of the summed coincidence spectrum of the measurements on the ten ^{165}Er sources. In addition to $\text{Ho} K\alpha$ x-ray random coincidences we see in Fig. 2(a) $\text{Tm} K\alpha$ x rays, mainly due to ^{171}Er , and $\text{Er} K\alpha$ x rays due to ^{166}Ho ($t_{1/2} = 26.2$ h). The latter contamination is due to neutron capture in ^{165}Ho , the daughter of ^{165}Er . The continuous background is due to ^{171}Er . The line shapes of the $\text{Tm} K\alpha$ x rays and the $\text{Er} K\alpha$ x rays have been obtained from separate coincidence measurements on, respectively, a source obtained by neutron bombardment of natural Er, and a ^{166}Ho source. The $\text{Er} K\alpha$ doublet was fitted in the coincidence spectrum by making use of the 80-keV gamma-ray transition in ^{166}Er . After subtraction of the random coincidences and of the contaminating lines and background, we obtain Fig. 2(b). The $\text{Ho} K\alpha_1^H$ line shows up clearly. The content of the line is $N_c = 97 \pm 31$ counts. The results of the measurement on ^{165}Er have also been summarized in Table I.

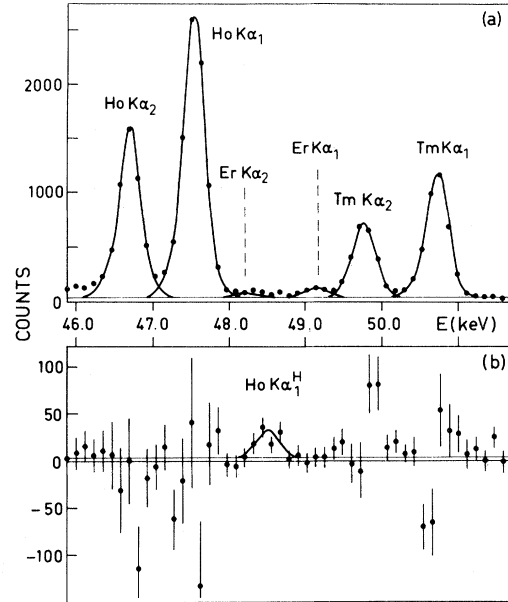


FIG. 2. (a) Ge coincidence spectrum of the $\text{Ho} K\alpha$ x-ray region; (b) *Idem*, after subtraction of random coincidences and coincidences due to contaminations.

The energy shifts of the $\text{Ta} K\alpha_1^H$ and $\text{Ho} K\alpha_1^H$ lines with respect to the corresponding diagram lines are (1026 ± 62) and (930 ± 70) eV, respectively. The errors are standard deviations. In Fig. 3 we show a compilation of experimental values of the energy shifts of $K\alpha_2^H$ and $K\alpha_1^H$ x-ray lines for $Z \geq 20$. The shifts have been normalized to the corresponding diagram $K\alpha_{1,2}$ line shifts for a change of the atomic number Z by one unit. These normalized values may be considered as ΔZ , the change in Z as a consequence of the second K -shell vacancy. The curves shown represent the shifts calculated by Chen *et al.*²⁰ The present results are in excellent agreement with the earlier data and with theory.

For a comparison of the P_{KK} values with other experimental results and with theory we consider Fig. 4. The upper solid curve is a smooth fit to the theoretical P_{KK} values for the isotopes ^{55}Fe , ^{71}Ge , ^{109}Cd , ^{131}Cs , ^{165}Er , and ^{169}Yb as obtained by Mukoyama *et al.*^{3,21}; the lower solid curve is a smooth fit to the $P_{KK}(\text{SO})$ values for the isotopes

TABLE I. Summary of experimental results.

	N_c	N_{NaI}	$\epsilon_c \epsilon_{\text{Ge}}$	P_{KK}
^{181}W series 1	73 ± 22	5.8×10^9	1.10×10^{-2}	$(2.4 \pm 0.7) \times 10^{-6}$
series 2	104 ± 40	8.3×10^9	1.10×10^{-2}	$(2.4 \pm 0.9) \times 10^{-6}$
^{165}Er	97 ± 31	2.1×10^9	1.18×10^{-2}	$(8.2 \pm 2.8) \times 10^{-6}$

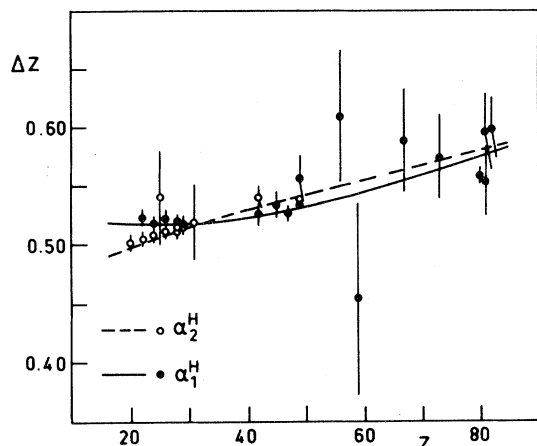


FIG. 3. Compilation of experimental values of energy shifts of $K\alpha_2^H$ and $K\alpha_1^H$ x-ray lines for $Z \geq 20$. Shifts have been normalized to the corresponding diagram $K\alpha_{1,2}$ line shifts for a change of Z by one unit: $\Delta Z = \Delta E(K\alpha_{1,2}^H - K\alpha_{1,2}^Z) / \Delta E(K\alpha_{1,2}^{Z+1} - K\alpha_{1,2}^Z)$. Points shown have been obtained from experiments on (references in order of increasing ΔZ value) Ca (Ref. 11), Ti, Cr (Ref. 12), ^{55}Fe (Ref. 13), Fe, Ni (Refs. 12 and 14), Cu, ^{71}Ge (Ref. 14), Mo (Ref. 15), ^{103}Pd (Ref. 16), ^{109}Cd (Ref. 4), $^{114\text{m}}\text{In}$ (Refs. 6 and 14), ^{137}Cs (Ref. 13), ^{141}Ce (Ref. 17), ^{165}Er and ^{181}W (present results), ^{199}Au (Ref. 18), ^{203}Hg (Refs. 19 and 13), and ^{207}Bi (Ref. 13). Curves shown represent theoretical values calculated by Chen *et al.*²⁰

^{55}Fe , ^{71}Ge , ^{131}Cs , and ^{165}Er , calculated by the same authors. Their calculations of P_{KK} and $P_{KK}(\text{SO})$ for ^{37}A have not been included since these values are completely off the smooth curves fitting the other results. The dashed curve is a smooth fit to the theoretical $P_{KK}(\text{SO})$ values for the isotopes ^{37}A , ^{71}Ge , ^{131}Cs , and ^{165}Er , as obtained by Intemann.¹ In all cases the difference between a theoretical P_{KK} or $P_{KK}(\text{SO})$ value used and the corresponding point on a curve is $\leq 10\%$ of the theoretical value.

The present result for ^{165}Er is in good agreement with the experimental result of Nagy *et al.*²⁵ and with theory. However, in the case of ^{181}W our experimental P_{KK} value of $(2.4 \pm 0.6) \times 10^{-6}$ is far below the theoretical curve. Therefore it seems that the earlier conclusion, that the theoretical P_{KK} values are too large for cases close upon the threshold, is confirmed. A critical remark is here in place. The assumption that the theoretical P_{KK} value for ^{181}W is given by the upper curve in Fig. 4 is based on the fact that this curve has a rather good fit to the theoretical values calculated so far. For a definitive conclusion a direct calculation of the theoretical P_{KK} value for ^{181}W is needed.

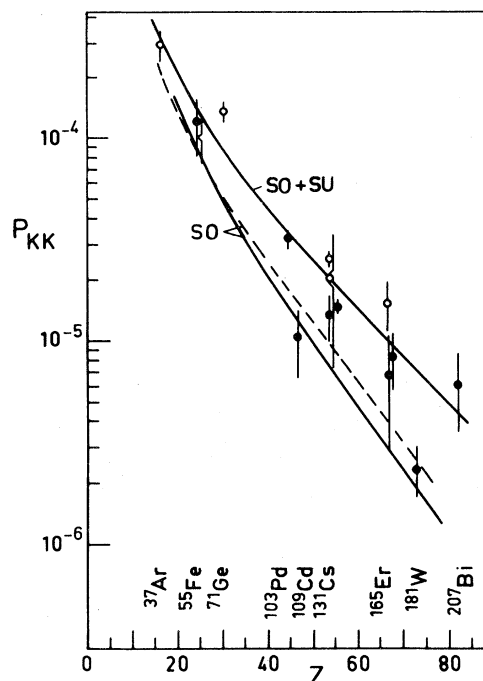


FIG. 4. Comparison of theoretical and experimental P_{KK} and $P_{KK}(\text{SO})$ values. The solid curves represent smooth fits to the theoretical values calculated by Mukoyama *et al.*^{3,21}; the dashed curve is a smooth fit to the theoretical $P_{KK}(\text{SO})$ values calculated by Intemann.¹ Isotopes for which the experimental values are shown are (references in order of increasing P_{KK} value) ^{37}Ar (Ref. 22), ^{55}Fe (Refs. 23 and 13), ^{71}Ge (Ref. 24), ^{103}Pd (Ref. 16), ^{109}Cd (Ref. 4), ^{131}Cs (Refs. 25–28), ^{165}Er (Ref. 25, present result, Ref. 29), ^{181}W (present result), ^{207}Bi (Ref. 30). Closed circles represent P_{KK} values obtained from semiconductor-detector experiments in which the hypersatellite lines of interest can be observed well separated; open circles represent P_{KK} values obtained from other experiments. Lower point for ^{55}Fe is an experimental $P_{KK}(\text{SO})$ value. The points are plotted at Z of the daughter nucleus.

For the present assuming that the discrepancy between experiment and theory is real, we plotted in Fig. 5 the ratios of the experimental P_{KK} 's and the theoretical P_{KK} 's as obtained from the upper curve in Fig. 4, $P_{KK}(\text{expt})/P_{KK}(\text{theor})$, as a function of the ratio of the Q value and twice the K binding energy, $\frac{1}{2}Q/K$. We attempted to draw a smooth curve through as many experimental points as possible. In doing so, we kept in mind that the result obtained from semiconductor-detector experiments (closed circles) must be considered more reliable as a consequence of the better possibility to discriminate against small contaminations in the source. In

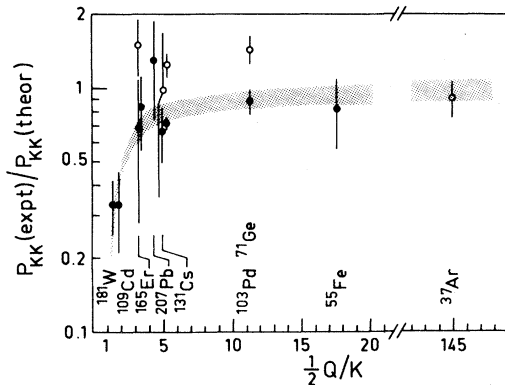


FIG. 5. Systematics in discrepancy between experiments and theory. Plotted are the ratios of the experimental and the theoretical (upper curve Fig. 4) P_{KK} values as a function of the ratio of the transition energy Q and the threshold energy $2K$. Band is a smooth fit to as many experimental points as possible.

addition, we took into account that the upper curve in Fig. 4 has deviations from the calculated theoretical values up to 10%. The band shown is the result. Only three experimental points out of 14 are off the band. The interesting feature of the band is that it has the simple analytical form

$$\frac{P_{KK}(\text{expt})}{P_{KK}(\text{theor})} \simeq 1 - \frac{2K}{Q}. \quad (2)$$

As yet an explanation for the observed discrepancy is not available.

ACKNOWLEDGMENTS

The authors are indebted to Dr. J. J. M. de Goeij and to Mrs. C. Zegers for their help in performing the chemical separations.

- ¹R. L. Intemann, *Proceedings of the Second International Conference on Inner Shell Ionization Phenomena—Invited Papers, 1976, Freiburg, West Germany*, edited by W. Melhorn and R. Brenn (Universität Freiburg, Freiburg, Germany, 1976).
- ²W. Bambynek, H. Behrens, M. H. Chen, B. Crasemann, M. L. Fitzpatrick, K. W. D. Ledingham, H. Genz, M. Mutterer, and R. L. Intemann, *Rev. Mod. Phys.* **49**, 77 (1977).
- ³T. Mukoyama, Y. Isozumi, T. Kitahara, and S. Shimizu, *Phys. Rev. C* **8**, 1308 (1973).
- ⁴C. W. E. van Eijk, J. Wijnhorst, and M. A. Popelier, *Phys. Rev. C* **19**, 1047 (1979).
- ⁵C. M. Lederer and V. S. Shirley, *Table of Isotopes* (Wiley, New York, 1978).
- ⁶C. W. E. van Eijk, J. Wijnhorst, and M. A. Popelier, *Phys. Rev. A* **24**, 854 (1981).
- ⁷D. Burch, L. Wilets, and W. E. Meyerhof, *Phys. Rev. A* **9**, 1007 (1974).
- ⁸H. Polkowska-Motrenko and R. Dybczynski, *J. Radioanal. Chem.* **59**, 31 (1980).
- ⁹T. Åberg, J. P. Briand, P. Chevallier, A. Chetioui, J. P. Rozet, M. Tavernier, and A. Touati, *J. Phys. B* **9**, 2815 (1976).
- ¹⁰W. Bambynek, B. Crasemann, R. W. Fink, H. U. Freund, H. Mark, C. D. Swift, R. E. Price, and P. Venugopala Rao, *Rev. Mod. Phys.* **44**, 716 (1972).
- ¹¹D. K. Olsen and C. F. Moore, *Phys. Rev. Lett.* **33**, 194 (1974).
- ¹²J. Ahopelto, E. Rantavuori, and O. Keski-Rahkonen, *Phys. Scr.* **20**, 71 (1979).
- ¹³J. P. Briand, P. Chevallier, A. Johnson, J. P. Rozet, M. Tavernier, and A. Touati, *Phys. Lett.* **49A**, 51 (1974).
- ¹⁴J. P. Briand, A. Touati, M. Frilley, P. Chevallier, A. Johnson, J. P. Rozet, M. Tavernier, S. Shafroth, and

- M. O. Krause, *J. Phys. B* **9**, 1055 (1976).
- ¹⁵S. I. Salem, *Phys. Rev. A* **21**, 858 (1980).
- ¹⁶C. W. E. van Eijk, J. Wijnhorst, and M. A. Popelier, *Phys. Rev. A* **20**, 1749 (1979).
- ¹⁷S. Ito, Y. Isozumi, and S. Shimizu, *Phys. Lett.* **59A**, 151 (1976).
- ¹⁸K. Schreckenbach, H. G. Börner, and J. P. Desclaux, *Phys. Lett.* **63A**, 330 (1977).
- ¹⁹J. P. Desclaux, Ch. Briançon, J. P. Thibaud, and R. J. Walen, *Phys. Rev. Lett.* **32**, 447 (1974).
- ²⁰M. H. Chen, B. Crasemann, and H. Marks, *Phys. Rev. A* **25**, 391 (1982).
- ²¹T. Mukoyama and S. Shimizu, *Phys. Rev. C* **13**, 377 (1976).
- ²²W. Neumann, in *Inner-Shell and X-Ray Physics of Atoms and Solids*, edited by D. J. Fabian, H. Kleinpoppen, and L. M. Watson (Plenum, New York, 1981), p. 289.
- ²³T. Kitahara and S. Shimizu, *Phys. Rev. C* **11**, 920 (1975).
- ²⁴M. Langevin, *J. Phys. Rad.* **19**, 34 (1958).
- ²⁵H. J. Nagy, G. Schupp, and R. R. Hurst, *Phys. Rev. C* **6**, 607 (1972).
- ²⁶Y. Isozumi, Ch. Briançon, and R. J. Walen, *Phys. Rev. C* **25**, 3078 (1982).
- ²⁷K. M. Smith, Ph.D. thesis, University of Glasgow, Scotland, 1964 (unpublished).
- ²⁸N. L. Lark and M. L. Perlman, *Phys. Rev.* **120**, 536 (1960).
- ²⁹H. Ryde, L. Persson, and K. Oelsner-Ryde, *Nucl. Phys.* **47**, 614 (1963).
- ³⁰J. P. Briand, R. P. Rozet, P. Chevallier, A. Chetioui, M. Tavernier, and A. Touati, *J. Phys. B* **13**, 4751 (1980).